A Phase Locked Loop for Molecular Communications and Computations

Chieh Lo, Yao-Jen Liang, *Member, IEEE*, and Kwang-Cheng Chen, *Fellow, IEEE*

***Abstract*—Molecular communication has been considered an emerging technology for both scientific and engineering interests, due to molecular biology and the need for nano-scale communication and computation systems. Molecular communication systems are widely analogue to electrical communication systems involving emitting molecules, diffused propagation of molecules, and reception of molecules, under stochastic characteristics of relatively slow propagation speed and short transmission range. To facilitate large-scale molecular information systems for the purpose of communication and computation, state-of-the-art explorations are generally assumed perfect alignment of timing among molecular devices and sub-systems. To reach synchronous condition in electronics, phase locked loop (PLL) is known to align timing or phase of waveforms. We extend PLL into molecular PLL (MPLL) consisting of basic elements such as molecular phase detector, molecular loop filter, and molecular voltage controlled oscillator. Due to stochastic nature of molecular diffusion, we further analyze MPLL in terms of the diffusion jitter, displacement, and the (particle or molecular) counting noise. Simulations verify the MPLL concept model, tracking performance, and robustness in operation.**

***Index Terms*—Nano-networks, molecular communications, particle diffusion, molecular phase-locked loop, biochemical device.**

I. Introduction

EMERGING significant interests to use molecules or particles carrying information are two-fold, to construct man-made nano-devices and subsequent nano-machines, or to synthesize biological or chemical devices and subsequent systems, for information transportation (i.e., communications) and information processing (i.e., computations). Moore's law in semiconductor has faced growth slowing due to the approaching limit of the photolithography [1]. Nano-technology has been considered to enable the realization of components in nano-scale ranging from 1 nm to 100 nm and is expected to have potential usage on many fields, including drug delivery, health monitoring, and cancer treatments [2]–[5]. Nano-machines of tiny components are able to accomplish some simple tasks at nano-scale (e.g., sensing, computation, actuation and communication) [6] and [7]. A typical nano-machine has too limited capability of performing complicated tasks, while a set of nano-machines can be engineered to communicate over a nano-network so as to fulfill more complex tasks [4]. For example, a system of molecular machines may provide a new method to interact with cells in medical care, to produce molecule-patterns for manufacturing, or to perform logic operation of molecular components in molecular computing [3] and [8]–[11]. This coordinated technology requires an efficient communication scheme among the communicating nano-machines from both the purpose of computing and networking. In nature, the above nano-networks already exist and are essential to share nano-scale information, such as the quorum sensing mechanism within which bacteria can communicate with each other by generating, emitting, and receiving small hormone-like molecules [12].

Nevertheless, synthetic biology emerges as a promising technological alternative in molecular communications and computations since the first biologically synthesized oscillator consisting of a cyclic daisy-chain through a multi-step negative feedback was reported in 2000, though sensitive to noise [13]. On top of basic functional blocks like switches and oscillators as a combination of activation and repression elements, engineering such a network of functional blocks into meaningful processing systems usually requires some kind of synchronization [14]. Such synchronization can be facilitated by chemical inducers or producing a signal corresponding to change of property, which is widely considered to communicate by quorum sensing [15]. State-of-the-art investigations are usually to study collective behaviors through extracellular communication by chemical signaling. Kuramoto model has been widely adopted to synchronization of large population of biochemical sinusoidal oscillators [16]. Furthermore, a synthesized gene network of global intercellular coupling can recreate complex cellular behaviors from biochemical reactions governing gene regulation and signaling pathway [17]. However, there exist some weak spots in such explorations, to motivate this piece of research on molecular phase-locked loop (MPLL):

- Synthesized biological information systems require interactions among basic elements and maintaining alignment of timing or phase to allow biological rhythms. It therefore suggests contraction of biochemical signals realized by the same kind of molecules or heterogeneous molecules under stochastic fluctuations or noise [18]. Interactive different equations or Fokker-Planck equation shall be employed to

Manuscript received November 18, 2013; revised April 28, 2014; accepted June 3, 2014. Date of publication November 6, 2014; date of current version December 31, 2014. This research is supported by the Ministry of Science and Technology under the contract 102-2221-E-002-016-MY2 and by the Ministry of Education.

C. Lo was with the Department of Electrical Engineering, National Taiwan University, Taiwan. He is now with the Department of Electrical and Computer Engineering, Carnegie Mellon University, Pittsburgh, PA 15213 (e-mail: chiehl@andrew.cmu.edu).

Y.-J. Liang is with the Department of Electrical Engineering, National Chiayi University, Chiayi 60004, Taiwan (e-mail: yjliang@mail.ncyu.edu.tw).

K.-C. Chen is with the Department of Electrical Engineering and the Graduated Institute of Communication Engineering, National Taiwan University, Taipei 10617, Taiwan, and also with SKKU, Seoul 110-745, Korea (e-mail: ckc@ntu.edu.tw).

Color versions of one or more of the figures in this paper are available online at http://ieeexplore.ieee.org.

Digital Object Identifier 10.1109/JSAC.2014.2367661

modeling, which was studied in detail in communication engineering as a PLL [19]. PLL model meets further precise engineering requirements of an element in large systems, than a simple oscillator.

- To achieve possibly precise digital computations and communication networks, precise understanding the alignment of molecular signals including quorum sensing is needed. Synthesis of biochemical PLL shall be a critical step in synthetic biology. Initial analysis on biochemical MPLL is not available, while understanding of behavior is obviously critical.

Generally speaking, in the information and communication technology (ICT) community, molecular communications act as an emerging methodology in information exchange and communication [3]–[6] and [20]–[27], due to post-silicon technology and molecular biology. Molecular communications may deliver information through transporting molecules in a massive fashion [4]. However, molecular communications have very different physical transmission characteristics from the conventional wireless communications in accordance with channel coding, synchronization, receiver detection, and other design considerations [5]. Molecular communications involve three basic processes: molecules/particles emission, molecules/particles propagation, and molecules/particles reception. Among these three processes, it is challenging to characterize molecular propagation [3]. For molecular communications, there are three main nano-network architectures based on molecules propagating across the medium: walkway-based, flow-based, and diffusion-based [4]. Diffusion-based molecular communications refers to the situation where molecules propagate through a particular diffusion in a fluidic medium [28]. For instance, calcium ion signaling, one of the most important communication mechanisms among living cells. In [4], a physical channel model with three phases of molecular communications, i.e., molecular emission, diffusion, and reception is introduced. In [20], achievable information rate for the molecular communications channel is investigated. In [21] and [22], the molecular noise in diffusion based molecular communications is modeled and examined. The information capacity of the relay channel in molecular communication system is analyzed in [23]. In [24], some transmission strategies for molecular communications channel are proposed based on in-sequence delivery of molecules. In [25] and [26], the molecular channel capacity is derived in an information theoretical approach and some necessary techniques for future nano-networks are also explored. In [27], the channel characteristics of molecular communications are derived based on the principles of Brownian motion and the respective communication rate is obtained. In [29], the authors proposed a binary digital communication system based on molecular diffusion and designed a detector following an communication-theoretic approach.

All existing research in molecular communication or computing assume that the synchronism is perfectly performed, by ignoring critical time jitter or phase error in computing, cuicuits, and communications. However, synchronization of molecular machines has been considered as an essential coordination functionality for molecular communications [11]. In this paper, we pioneer the investigations in MPLL by modeling the biochemical/physical molecular diffusion process for molecular communications, circuitries, and computations. The proposed MPLL modeling is extensively examined by characterizing its basic three components, i.e., molecular PD (MPD), molecular LF (MLF), and molecular VCO (MVCO). Thorough numerical results are described for the entire PLL in term of the acquisition time, tracking performance and robustness.

The remainder of this paper is organized as follows. In Section II, we briefly review the diffusion process based on the Flick's second law. In Section III, we introduce the PLL system model for the diffusion-based molecular communication. In Section IV, we analysis the steady-state error, loop gain, loop bandwidth, and acquisition time for the proposed PLL diffusion model under the assumption of deterministic diffusion model. In Section V, the randomness of diffusion channel is considered and some stochastic behaviors, like the diffusion jitter, the displacement, and the molcule counting noise are observed. Finally, some concluding remarks and future research topics are given in Section VI.

II. Characterizing the Diffusion Process

Before stepping into the proposed system model, we give a brief review to the diffusion process that is fundamentally different from electromagnetic communications. The diffusion process is stochastic and the motion of a molecule follows a random walk. Although the space of the diffusion process in a fluid medium has multiple dimensions, without loss of generality, we start from the one-dimensional case. We suppose that a molecule is released in a static fluid medium at position x_0 and time t_0. Let $X(t)$ and $P_x(x,t;x_0,t_0)$ denote the position of the molecule at time t and its respective probability density function (PDF), respectively. A specific molecule in a static fluid medium diffuses with equal probability in either positive or negative directions. We further assume that the quantity of the emitted molecules is Q at a specific time instant and these molecules are modeled as independently and identically distributed random variables through the diffusion process. The PDF $P_x(x,t;x_0,t_0)$ can then be characterized by the Fick's second Law [30]

$$Q\frac{\partial}{\partial t}P_X(x,t;x_0,t_0) = QD\frac{\partial^2}{\partial x^2}P_X(x,t;x_0,t_0), \qquad (1)$$

where D is the diffusion constant, which depends on the viscosity of the fluid medium with a constant velocity v ($v > 0$). Without loss of generality, we assume that this molecule is released at the origin. The PDF of the molecule position can be simplified to $P_X(x,t;0,0)$ and denoted hereinafter as $P_X(x,t)$. The partial differential equation (PDE) of $P_X(x,t)$ can be written as [31]

$$Q\frac{\partial}{\partial t}P_X(x,t) = Q\left(D\frac{\partial^2}{\partial x^2} + v\frac{\partial}{\partial x}\right)P_X(x,t). \qquad (2)$$

Assume that there is no absorbing boundary in the receiver end and the PDE composes two boundary condition $P_X(x,0) = \delta(x)$ and $P_X(\pm\infty,t) = 0$, then $P_X(x,t)$ can be obtained as

$$P_X(x,t) = \frac{1}{\sqrt{4\pi Dt}}exp\left(-\frac{(x-vt)^2}{4Dt}\right). \qquad (3)$$

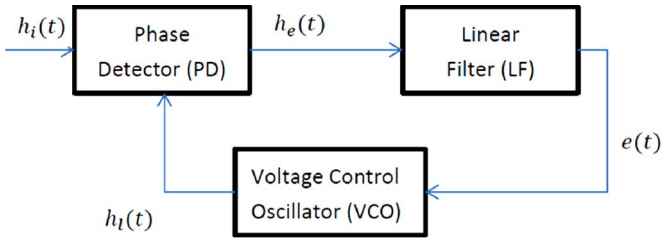

Fig. 1. Classic Phase locked loop.

Afterward, the fluid velocity v is assumed to be zero for simplicity of derivation.

III. System Model

The diffusion-based molecular communication generally consists of three phases of operation, i.e., molecular emission, diffusion, and reception. Without loss of generality, the transmitter is assumed to be located at the origin and the modulated signal consists of N_t charged molecules. The receiver is at a designate distance from the transmitter. To retrieve the information emitted from the transmitter, the receiver is required to detect the concentration of the molecular around its neighborhood and release the same amount of concentration of the opposite charged molecules. The arrival times of the molecules, however, are hard to be predicted. Subsequently, the receiver requires a well-designed mechanism, to react fast for the incoming molecules, and to track the molecular signal waveform.

In traditional communication systems, the synchronization of the incoming signal is realized by a PLL as shown in Fig. 1. The basic operation of the PLL consists of three elements: PD, LF, and VCO. The PD generates an error difference signal according to the phase difference of the input signal and the locally generated signal to drive VCO in an appropriate way. Although variations of PLL exist [32], the same principle applies. This concept motivates us to investigate PLL in the diffusion-based molecular communications, circuitries, and computations.

A. Loop Components

To explicitly demonstrate the signal which MPLL targets at to lock, we simplify the signals by two kinds of molecules/particles as A^+ and B^- to represent general chemical reactions (i.e., $A^+ + B^- \rightarrow AB$). The molecular PLL then tries to lock the locally generated molecules B^- with the arrived molecules A^+ for decoding of the transmitted signals as shown in Fig. 2(b).

For the purpose of simplicity in our diffusion model, the receiver generates opposite charged molecules or any corresponding chemical reactants to track the input charged molecules, which can be easily extended to general biochemical reaction processes [18] but phase locking mechanism is overlooked in literature. The concentration of the locally generated molecules is determined by the loop locating at the receiver. This diffusion model contains a phase detector similar to the one of a classic PLL. An easy way to comprehend by considering one positive molecule and one negative molecule to form a new

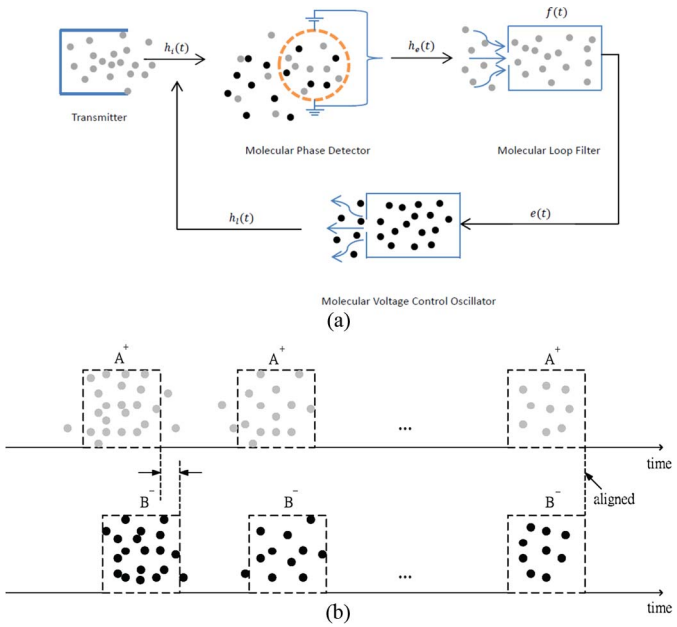

Fig. 2. Molecular PLL model for the first-order loop. (a) The gray spots represent input molecules/particles and the black spots represent local generated molecules/particles. (b) Molecular PD to align the input molecules/particles A^+ and the locally generated molecules/particles B^- during the process of MPLL operation to align two signal waveforms composed of A^+ molecules and B^- molecules.

complex compound,[1] and the error signal is thus equivalent to the amount of net charges with either positive or negative polarity. The MPD quantitatively compares the amount of two molecules that we use A^+ and B^- as the simplest scenario, therefore, MPD here degenerate to a "charge detector", without loss of generality. The molecular loop filter in MPLL intends to allow possible further function in the future, while we only keep the simplest form of low-pass filter in this paper. The molecular VCO adaptively generates molecules in a proper way trying to lock molecular "signals", which might require more sophisticated wet-laboratory chemical realization. Since we deal with $A^+ + B^- \rightarrow AB$ as the simplest case, it simply behaves like a VCO using electrical measurement in this paper, but generally not confined to voltage nor to oscillation under chemical measurement and operation.

B. Loop Formulation

We use the definition of molecule flux as the net molecule concentration leaving/entering a process per unit time [4]. As shown in Fig. 2(a), the arrived molecular concentration $h_i(t)$ biochemically reacted with the locally generated concentration $h_l(t)$. Then the error concentration $h_e(t)$, which stands for the net charge after reaction, enters the molecular loop filter (MLF) and $e(t)$ is outputted, that is, $e(t)$ can be represented as the convolutional result of $h_i(t)$ and $f(t)$, which stands for the transfer function of MLF. Subsequently $e(t)$ roles as a molecule flux to drive the molecular VCO (MVCO) and is defined as

[1]The generalization to molecular communications composed of complicated reactants is straightforward and the description is omitted here for space limitation.

the time derivative $dh_l(t)/dt$ of output molecule concentration $h_l(t)$. The above phenomenons are represented by mathematical equations as follows. The error concentration is

$$h_e(t) = h_i(t) - h_l(t). \tag{4}$$

The input signal $e(t)$ to the MVCO can be written as

$$e(t) = k_1 \int_0^t h_e(\tau) f(t-\tau)\, d\tau, \tag{5}$$

where k_1 denotes the gain of the loop filter. The locally generated signal $h_l(t)$ can be related to the MVCO as

$$\frac{\partial h_l(t)}{\partial t} = k_2 e(t). \tag{6}$$

where k_2 denotes the gain of the VCO.

Above equations aptly describe the loop behavior of a MPLL. However, some modifications should be included in our MPLL scheme. Since the MPD detects the net charge of the input signal and output signal, the issue of chemical reaction should be taken into consideration. At the MPD, the input molecules A^+ and the locally generated molecules B^- react and form a complex compound C (or simply AB), that is,

$$A^+ + B^- \rightarrow C. \tag{7}$$

The above chemical reaction yields, using the law of mass-action [33], the following dynamics:

$$\frac{d[A]}{dt} = -k_f[A][B] \tag{8}$$

$$\frac{d[B]}{dt} = -k_f[A][B] \tag{9}$$

where k_f is the forward rate and $[\cdot]$ denotes the concentration of the specific species.

Here we replace [A] and [B] with $h_i(t)$ and $h_l(t)$ in (8) and (9), respectively and substitute them into (4)–(6). Combined with Fick's second Law and the law of mass action, (6) can be reformulated as

$$\frac{\partial h_l(x,t)}{\partial t} = \underbrace{D_l \frac{\partial^2 h_l(x,t)}{\partial x^2}}_{Fick's\ Second\ Law} + \underbrace{k_2 e(x,t)}_{MVCO} - \underbrace{k_f h_i(x,t) h_l(x,t)}_{Mass\ Action}. \tag{10}$$

After some straightforward manipulations, we can acquire the following equation

$$\frac{\partial \left(h_i(x,t) - h_e(x,t)\right)}{\partial t} = D_l \frac{\partial^2 (h_i(x,t) - h_e(x,t))}{\partial x^2} + k_2 k_1 h_e(x,t) - k_f h_i(x,t) h_l(x,t). \tag{11}$$

From (4), (5), and (11) and with the assumption that $f(t) = \delta(t)$ (first order loop), we obtain

$$\frac{\partial h_i(x,t)}{\partial t} - D_i \frac{\partial^2 h_i(x,t)}{\partial x^2} = \frac{\partial h_e(x,t)}{\partial t} - D_l \frac{\partial^2 h_e(x,t)}{\partial x^2} + K h_e(x,t) - k_f h_i(x,t) h_l(x,t) \tag{12}$$

where $K = k_1 k_2$ denotes the overall gain of the loop. The input signal also follows the diffusion-reaction equation [34]:

$$\frac{\partial h_i(x,t)}{\partial t} = D_i \frac{\partial^2 h_i(x,t)}{\partial x^2} - k_f h_i(x,t) h_l(x,t). \tag{13}$$

Consider a homogeneous medium and assume that the equivalent ions of the input signal and locally generated signal have the same diffusion coefficient, i.e., $D_l = D_i = D$, (12) can be simplified as

$$\frac{\partial h_e(x,t)}{\partial t} = D \frac{\partial^2 h_e(x,t)}{\partial x^2} - K h_e(x,t). \tag{14}$$

It is worthy noting that under the assumption of $f(t) = \delta(t)$ and $D_l = D_i = D$, the error signal $h_e(x,t)$ is no longer dependent of the forward rate k_f in (8) and (9). The solution of (14) can easily be deduced as [35]

$$h_e(x,t) = \frac{M}{\sqrt{4\pi D t}} e^{-Kt} e^{-\frac{x^2}{4Dt}}, \tag{15}$$

with initial conditions $h_e(x,0) = M$ and $h_e(\pm\infty, t) = 0$. The marginal pdf $h_e(t)$ can be consequently expressed as

$$\int_x h_e(t,x)\, dx = M e^{-Kt} \tag{16}$$

From (16), it can be revealed that the averaged error in the entire space eventually tends to zero as time passed.

IV. Performance Analysis

In Section III, the loop equation is derived and the stochastic behavior of the diffusion equation is also examined. Here, we discuss the loop characteristics and give some insights into each of them.

A. Steady-State Errors

We first examine the error signal of the signal. From (15), it can be easily shown that

$$\lim_{t\to\infty} h_e(t) = 0.$$

The error signal finally approached to zero, that is, the input and locally generated signals are synchronized.

B. Loop Gain

The loop gain in traditional phase lock loop plays an important role in tracking and acquisition phases. The higher the loop gain is, the faster PLL can lock the phase at the cost of potentially sacrificing stability.

Consider a PLL with θ_i, θ_l, $\theta_e = \theta_i - \theta_l$ represent the input phase, locally generated phase and phase error, respectively. The phase error related to the loop shown in Fig. 1 can be expressed as

$$\frac{d\theta_e(t)}{dt} = \frac{d\theta_i}{dt} - AK \int_0^t f(t-\tau) \sin\left(\theta_e(\tau)\right) \mathrm{d}\tau, \tag{17}$$

where A is the amplitude of the input sinusoidal, K is the overall loop gain and $f(t)$ the filter function. Leveraging the approximation ($\sin(\theta_e(t)) \approx \theta_e(t)$, $\theta_e(t) \ll 1$), the first order approximation of (17) becomes

$$\frac{d\theta_e(t)}{dt} = \frac{d\theta_i}{dt} - AK\theta_e(t). \tag{18}$$

Set $\frac{d\theta_e(t)}{dt} = 0$, i.e., the loop is locked, we can obtain

$$\theta_e(t) = \frac{d\theta_i}{dt}\frac{1}{AK} \tag{19}$$

Let $\frac{\partial h_e(x,t)}{\partial t} = 0$ in (14), we can obtain

$$h_e(x,t) = D\frac{\partial^2 h_e(x,t)}{\partial t^2}\frac{1}{K}. \tag{20}$$

As the loop gain grows, the acquisition of the loop can be accomplished quickly. From (19) and (20), the phase error (signal) in traditional phase tracking scheme is proportional to the first derivative of the input signal; while in our proposed model, that is proportional to the second derivative of the error signal itself. In usual cases, the amplitude of the second derivative is smaller than the first derivative even it also depends on the signal type considered. Therefore, an appropriate loop gain is an important factor in the MPLL design.

Now we examine how loop gain affect the locally generated signal in two cases. One is a short range transmission of calcium molecules with $D = 10^{-6}$ cm^2/s, $r = 20$ μm and the other is a long range transmission of calcium molecules with $D = 0.4$ cm^2/s, $r = 2$ cm. Fig. 3(a) and (b) show the locally generated signals with different loop gains in short and long ranges, respectively. In short range transmission, the locally generated signal reaches its peak at about 1.5 sec, which is smaller than the long range transmission (it reaches its peak at 4.0 sec). While, with the same loop gain, the long range transmission tracks signal better than the short range one. Furthermore, at around loop gain $(K) = 20$ dB the locally generated signals in both cases are almost identical to their respective input signals. Thus, a suitable designation of loop gain for a specific diffusion coefficients, which relies on the molecule species and environment, also plays an important role in the MPLL design.

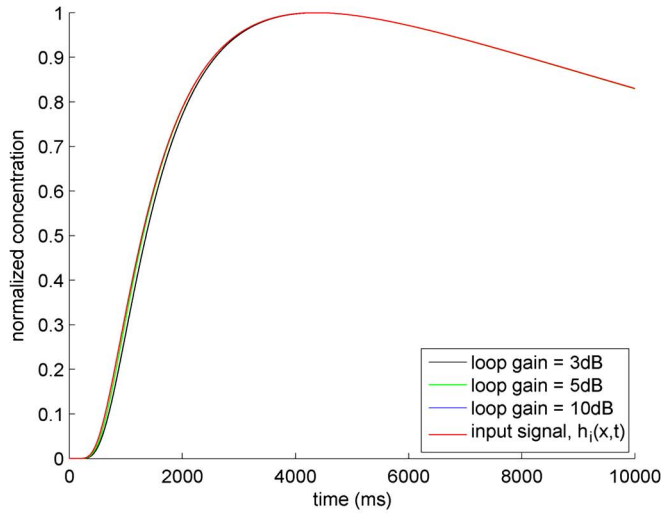

Fig. 3. Local generated signal with different loop gain (K) in (a) long range and (b) short range molecular transmissions.

C. S Curve of The Phase Detector

The S curve in a traditional phase-locked loop performs linearly as given a small amount of the phase error. In our proposed model, however, we assume that the phase detector can operates linearly with unlimited net charges. Under this assumption, the output signal of MPD may go high from the stable level. However, for practical design consideration, the S curve of the phase detector should have limited output level not only to ensure the stability of the loop but also to reduce the design cost. The transmission rate of the molecules modulated at the transmitter is assume fixed and well known at both the transmitter and receiver. Besides, the maximal magnitude of the incoming signal would determine the range of the error signal and act as a key factor for characterizing the S curve of the phase detector. The occurred time of the maximal magnitude of the diffusion process can be obtained by differentiating (3) with respect to t, that is

$$t_{max} = \frac{x^2}{2dD},$$

where d is the dimension. The respectively maximal value is thus became as

$$h_{i\_max} = N_t\left(\frac{d}{2\pi e}\right)^{d/2}\frac{1}{x}. \tag{21}$$

For the diffusion motion on the line considered, here we have $d = 1$. We further assume that the receiver knows the magnitude of the signal diffused from the transmitter and the error signalranges from $-h_{i\_max}$ to h_{i_max}. Once the error exceeds above range, the phase detector should limit the output signal otherwise the loop may not track the input signal. However, the distance between transmitter and receiver is unknown. The estimation of the concentration before tracking is necessary and should be used to initialize the parameters of the S curve of the MPD.

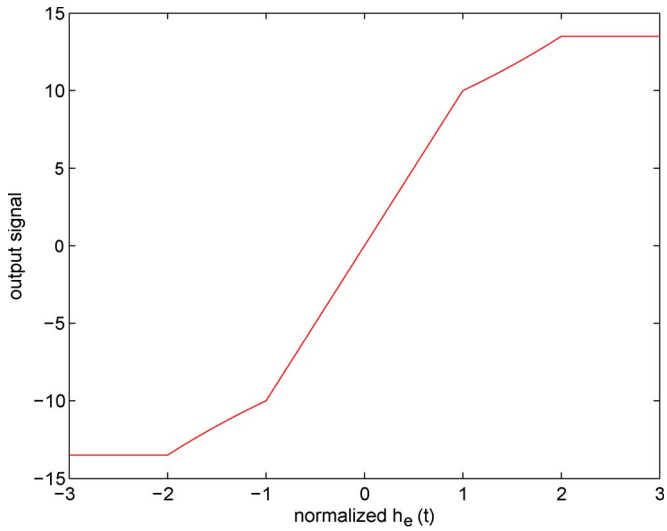

Fig. 4. S curve of the molecular phase detector.

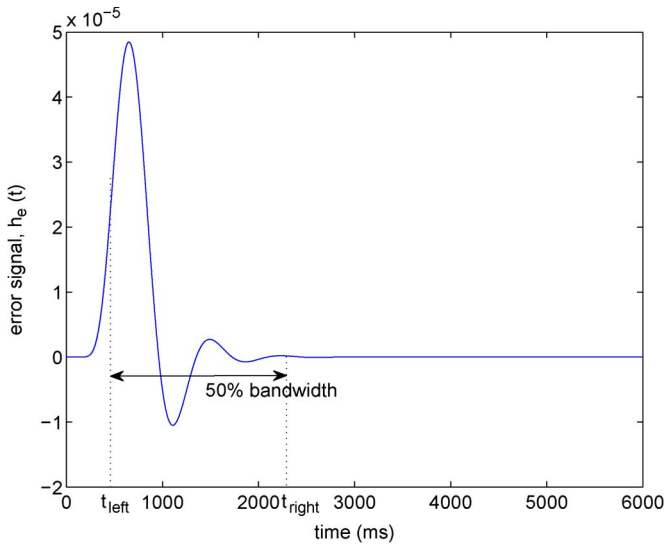

Fig. 5. Acquisition time defined by the 50% bandwith of the error signal $h_e(t)$, (24), (25).

The corresponding S curve of the MPD is shown in Fig. 4, where the x-axis is normalized with respect to the h_{i_max}. Within the region $+h_{i\_max} \sim -h_{i\_max}$, the MPD operates linearly with a constant slope. Outside this region, it operates nonlinearly with moderate slope until it reaches the flat region. The flat region limits the output signal to certain value when the input error signal is too large so as to ensure the stability of tracking.

D. Acquisition

In the settling time analysis of a classic PLL, given the center frequency of the VCO f_c, the lock-in range is defined as the input frequency deviation in which the PLL locks in the linear range of the phase detector. While pull-in range is defined as the maximal output frequency range that allow the PLL to lock.

However, in the molecular case, the center and natural frequency of a MPLL is difficult to be defined, thus we turn to analysis theacquisition time[2] alternatively. Our diffusion loop is initially assumed unlocked, the time that the lock-in process takes is defined as the acquisition time. From (15), it can be observed that the error signal follows a diffusion-like model with an exponential decay factor e^{-Kt}. The 50% bandwidth of the signal is defined according to the peak of the error signal intersecting with the time axis at two points. The acquisition time is defined as the time difference of these two points. Differentiating the error signal $h_e(t)$ in (15) with respect to the time t and setting it to zero, we have

$$t_{peak} = \frac{-D + \sqrt{D^2 + 4DKx^2}}{4DK} \tag{22}$$

$$h_e^{peak}(x) = \frac{M}{\sqrt{4\pi D t_{peak}}} e^{-Kt_{peak}} e^{-\frac{x^2}{4Dt_{peak}}}. \tag{23}$$

Let

$$h_e(x,t) = \frac{1}{2} h_e^{peak}(x) \tag{24}$$

and substitute it into (15). The acquisition time is then obtained as

$$t_{acquisition} = t_{right} - t_{left}, \tag{25}$$

where $t_{right} > t_{left}$ are the two solutions of t in (24). Then we use Fig. 5 to illustrate the 50% bandwith and acquisition time in (24) and (25), respectively. Where t_{left} is determined by the time occurred at 50% magnitude of the first peak $h_e(x,t)$, which leaves from zero magnitude; while t_{right} is the time occurred at the 50% magnitude of the last peak returning to zero.

V. Stochastic Analysis

The stochastic behavior of the diffusion process can be considered analogous to the noise effect in the classic PLL, while the noise effect of the former is much more severe than the latter and cannot be ignored. Compared to telecommunications, the speed and range of molecular communications is slow and short, and varies depending on the molecular species, the mechanism used, and operating environment [10]. Furthermore, molecular communications experience large delay jitters due to the stochastic movements of molecules, which suggests the need of the stochastic characteristics for the molecular communications. Here we consider three different stochastic noises. One is the delay jitter cased by the Brownian motion of the diffusion molecules, wherein certain delay and/or jitter exists among the different molecules. The jitter may also come from the chemical reaction process. For the molecules to react at certain degrees, the reaction time is moderate and can be viewed as a jitter to the loop. Another source comes from the displacement of the MPD and MVCO within a MPLL. Since the chemical reaction and local signal generation may occur at different positions, the distance would affect the diffusion behavior and defer the following charge detection. The last source of the random behavior comes from the measurement of the error signal. This discrete measurement would accompany some counting noise. Finally, these three sources of the stochastic noise are assumed to be independent to each other and will be discussed in the following.

[2]Loop bandwidth is proportional to the inverse of the acquisition time in general.

A. Jitter in Diffusion Loop

In chemical reaction, both the input signal and the locally generated signal are composed of chemical molecules. The chemical reaction would require a large propagation delay, since the chemical molecules have to propagate to meet together and then trigger a reaction. In addition, the arrival time between the input signal and the locally generated signal may have certain amount of time shift due to the random behavior of individual molecules. This also induces some extra of delay and jitter. Considering above two issues, we assume the total time shift to be composed of a fixed amount of delay and a random jitter.

Let τ be the chemical reaction delay. Then (4) incorporated with the reaction delay τ can be expressed as

$$h_e(x,t-\tau) = h_i(x,t-\tau) - h_l(x,t-\tau). \tag{26}$$

Assuming τ is small enough due to a dense concentration of input molecules, and approximating $h_i(x,t-\tau) = h_i(x,t) - \tau\frac{\partial h_i(x,t)}{\partial t}$ and $h_l(x,t-\tau) = h_l(x,t) - \tau\frac{\partial h_l(x,t)}{\partial t}$,[3] we can rewrite (26) as

$$h_e(x,t-\tau) = h_e(x,t) - \tau\frac{\partial h_e(x,t)}{\partial t}. \tag{27}$$

Consequently, the delayed version of the error signal in (14), $h_{e\_delay}(x,t)$, with $f(t)=\delta(t)$ can be reformulated as

$$(1+K\tau)\frac{\partial h_{e\_delay}(x,t)}{\partial t} = D\frac{\partial^2 h_{e\_delay}(x,t)}{\partial x^2} - Kh_{e\_delay}(x,t). \tag{28}$$

After some straightforward manipulations, the solution of (28) can be derived as

$$h_{e\_delay}(x,t) = \frac{M}{\sqrt{4\pi D't}} e^{-\frac{K}{1+K\tau}t} e^{-\frac{x^2}{4D't}}, \tag{29}$$

where $D' = \frac{D}{1+K\tau}$.

From (29), the factor $1+K\tau$ affects the operation of the loop. Since the delay factor τ is assumed to be very small, the main contribution to $1+K\tau$ would be the loop gain, K. Here we examine two extreme cases as follows. If $K\tau \ll 1$, (29) degenerates to (15). On the other hand, as $K\tau \gg 1$, (29) becomes

$$h_{e\_delay}(x,t) = \frac{M}{\sqrt{4\pi D''t}} e^{-\frac{1}{\tau}t} e^{-\frac{x^2}{4D''t}}, \tag{30}$$

where $D'' = \frac{D}{K\tau}$.

It is worthy considering the time when the error signal reaches its peak and the corresponding amplitude. By differentiating the error signal $h_{e\_delay}(t)$ in (29) with respect to the time t and setting it to zero, we get the respective peak time and the peak amplitude as

$$t_{peak\_delay} = \frac{-D' \pm \sqrt{D'^2 + 4D'K'x^2}}{4D'K'}, \tag{31}$$

$$h^{peak}_{e\_delay}(x) = \frac{M}{\sqrt{4\pi D t_{peak\_delay}}} e^{-Kt_{peak\_delay}} e^{-\frac{x^2}{4Dt_{peak\_delay}}}. \tag{32}$$

where $K' = \frac{K}{1+K\tau}$.

From (23) and (32), we calculate the ratio of the peak amplitude without delay to that with delay as

$$\frac{h^{peak}_e(x)}{h^{peak}_{e\_delay}(x)} = \frac{\sqrt{D't_{peak\_delay}}}{\sqrt{Dt_{peak}}} \cdot \exp(-Kt_{peak} + K't_{peak\_delay}) \cdot \exp\left(-x^2\left(\frac{1}{4Dt_{peak}} - \frac{1}{4D't_{peak\_delay}}\right)\right) = 1. \tag{33}$$

The last equality of (33) comes from that each term on the right hand side of the first equal sign of (33) equals to unity. Fig. 6 confirms the above derivations with certain numerical round-off error in evaluating (15) and (29). Thus, delay only affects the peak-to-peak delay, i.e., the difference of t_{peak_delay} and t_{peak} as

$$t_{peak-to-peak} = t_{peak\_delay} - t_{peak}. \tag{34}$$

The jitter, caused by the chemical reaction and the generated signal, would also affect the convergence of the error signal. Take Fig. 6 as an example, the chemical delay τ is set to 0.01 s but the peak-to-peak delay is about 0.15 s. This nonlinearity of the $t_{peak-to-peak}$ can be analyzed by using the phase plane methods, which is out of the scope of this paper. Comparing the two error signals in Fig. 6, we can find that the shape of error signal is spread by the delay. The main cause comes from (29), wherein the gain-delay product $(K\tau)$ makes the exponential term with less deep slope. The tolerance of the $t_{peak-to-peak}$, the peak magnitude of the error signal and the lasting time of the error signal are trade-offs in system design consideration. In

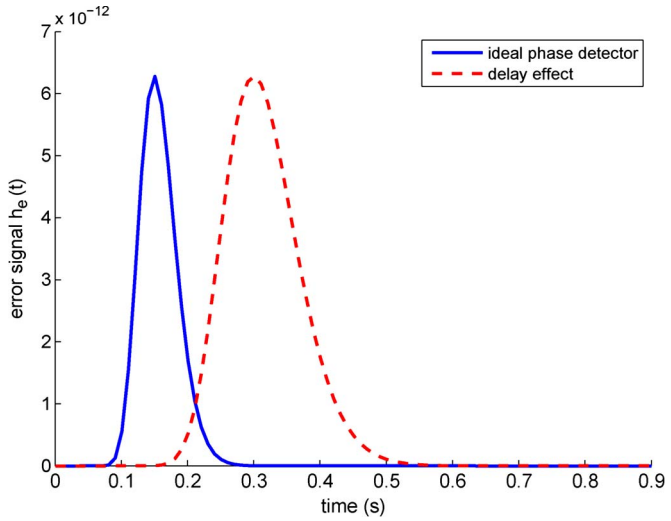

Fig. 6. Jitter affects the error signal on delay from the one of an ideal phase detector.

[3]The first order of Taylor series expansion is applied here.

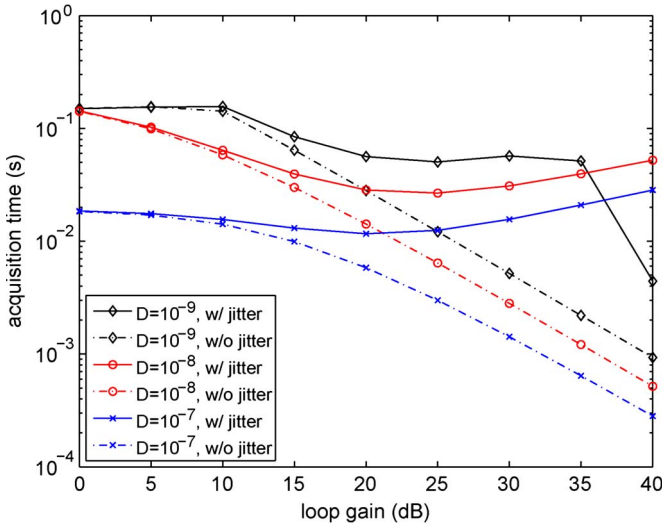

Fig. 7. Acquisition time of jitter effect among various diffusion coefficients.

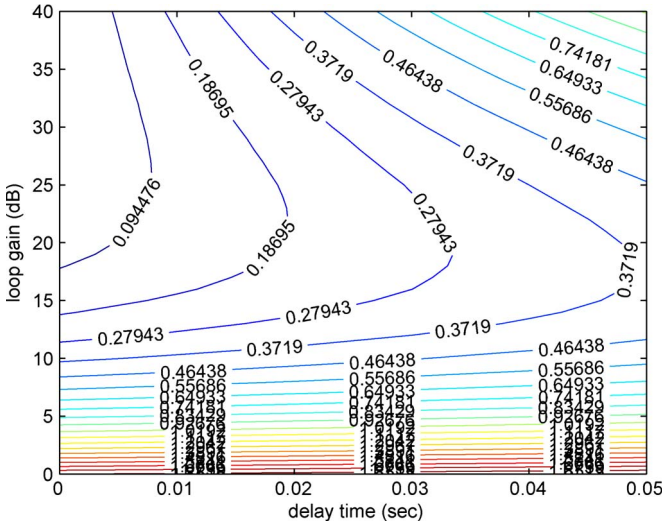

Fig. 8. Contour of acquisition time with respect to different delays and loop gains with the delay time ranges from 0 to 0.05 and the loop gain from 0 to 40 dB and all other settings the same as in Fig. 7.

a certain specification, a system may trade the magnitude of the error signal for a larger tolerance of $t_{peak-to-peak}$.

Similar to the acquisition time definition in (25), here we re-examine the acquisition time of the loop with the delay effect. In Fig. 7, three different diffusion coefficients ($D = 10^{-9}, 10^{-8}, 10^{-7}$ m^2/s) with same propagation distance $x = 20$ μm are examined. Consider the case without jitter, the acquisition time decreases as the loop gain of the molecular PLL grows for all three cases. While in the case with jitter equalled to 0.01 sec, the acquisition time increases as the loop gain exceeds about 25 dB and the increasing slope becomes deeper for a larger diffusion coefficient. This phenomenon shows that loop bandwidth/acquisition time worsens with jitter effect especially the diffusion speed is fast, which consists the usual knowledge of the chemical diffusion. Furthermore, Fig. 8 draws the contour of the acquisition time with the delay time ranges from 0 to 0.05 and the loop gain from 0 to 40 dB and all other settings the same as in Fig. 7. At fixed delay time, as loop gain increases the acquisition time decreases. On the contrary, at a given loop gain, the acquisition time grows as delay time increases. Furthermore, the contours loosen at larger loop gain intuitively, this means that a large loop gain improves the convergence. The diffusion coefficient depends on the molecule characteristics and the environment for propagation. The acquisition time and/or loop bandwidth is shown not always positive related to the loop gain, thus a careful off-line designation of loop gain is required for different chemical species and different operating environments.

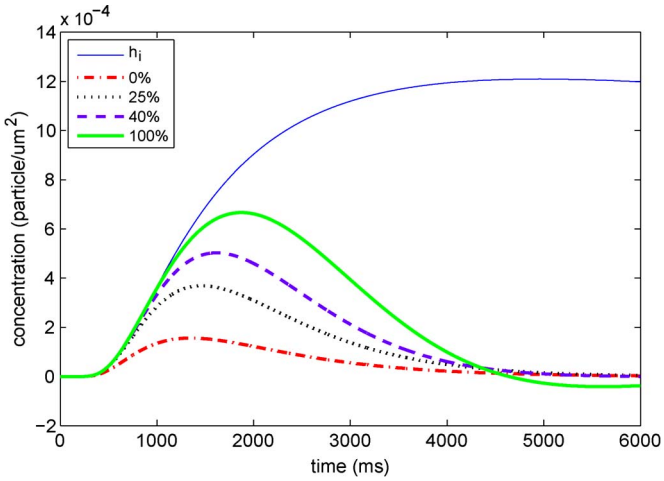

Fig. 9. The displacement effect for the locally generated signal h_l with loop gain $= 0$ dB, and various displacements normalized to the transmitter-receiver distance.

B. Displacement Between the MPD and MVCO

The chemical reaction may occur as soon as the input molecules meet the locally generated molecules regardless of a designate position. Thus, the distance between the MPD and MVCO should be considered as another source of stochastic noise. Let the positions of local signal generation and chemical reaction be x and $x + \triangle x$, respectively, where $\triangle x$ denotes the displacement. Thus the VCO generating equation (6) can be extended to the following differential

$$\frac{\partial h_l(x,t)}{\partial t} = k_2 e(x,t), \tag{35}$$

with

$$e(x,t) = h_l(x + \triangle x, t) - h_i(x,t). \tag{36}$$

The above differential equation is generally not tractable. Thus, we alternatively search the solution by numerical methods. The normalized average displacement, i.e., $\mathrm{E}(\triangle x)/|x|$ is used in the numerical evaluations. Figs. 9 and 10 show the displacement effect of the locally generated signal at loop gain equaled to 0 dB and 10 dB, respectively. In Fig. 9, the error signal increases in magnitude as displacement grows, however, the loop remains stable even after several loop cycles. While in Fig. 10, as the loop gain is enlarged to 10 dB, the displacement of 100% will drive the error signal high from stability, thus the loop behaves like a positive feedback loop. The acquisition time with 25% displacement error is about 5 times of that with 0% displacement. It is also required for an off-line designation of loop gain in accordance to various displacements encountered.

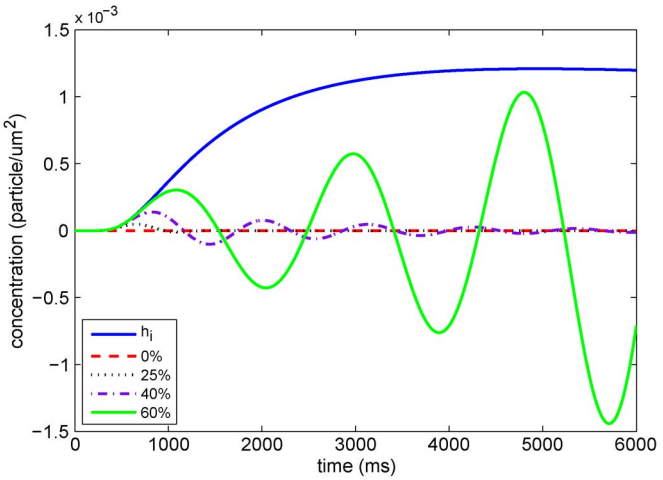

Fig. 10. The displacement effect for the locally generated signal h_l with loop gain $= 10$ dB, and various displacements normalized to the transmitter-receiver distance.

C. Molecule Counting Noise

In the above two subsections, we study the diffusion-based macroscopic stochastic on delay jitter and position displacement. Here we examine the most relevant microscopic noise, the molecule counting noise, to capture the affected phenomenons in molecular propagation. The collective behavior of molecules propagating through the channel can be well described by the Fick's second law, which is appropriate for large number of molecules. The number of molecules may not be accurate by directly multiplying the multiplied concentration with the detection volume, since the counting noise arises in the discrete nature of the molecules. This phenomenon can critically affect the diffusion process in MPLL.

Supposed the detection space at the receiver is countable and generally its volume is much smaller compare to the molecule propagation space. The detection space with finite volume is denoted by V_{space} and the number of the measured molecules is denoted by $N_a(t)$. The molecule's movement is assumed to follow the Brownian motion. To properly model the random process, several additional assumptions are utilized:

- In the detection, the molecular concentration $h_i(t)$ is supposed to be uniformly distributed.
- The expected number of detected molecules $E[N_a(t)]$ are calculated as concentration $h_i(t)$ multiplied by the reception space V_{space}

$$E\left[N_a(t)\right] = h_i(t)V_{space}. \tag{37}$$

- The molecule can only occupy one particular position in the space at one time instant t. Mathematically speaking, the probability that two different molecules occupy the same position is zero, that is

$$\lim_{\Delta x \to 0} \text{Prob}\left[|h_i(x+\Delta x,t) - h_i(x,t))| > \epsilon\right] \to 0, \tag{38}$$

  where $\epsilon > 0$.
- Because of the independence of the Brownian motion, the distribution of the distance among different molecules is also independent to the distribution of other distance. For instance, the distribution of the distance between molecules m_1 and m_2 is independent of the distribution of the distance between molecules m_1 and m_3, where m_i stands for the ith molecule. This implies that the location of a molecule is independent of the location of other molecules. In other words, the event of the location of the molecules in a space is memoryless.

Under these assumptions, the actual number of the molecules in the detection space can be modeled by a nonhomogeneous Poisson counting process, whose rate of occurrence corresponds to the expected molecule concentration [21], that is

$$\frac{N_a(t)}{V_{space}} \sim \text{Poisson}\left(h_i(t)\right). \tag{39}$$

As a result, the number of molecules $N_a(t)$ measured in the detection space over a time interval t is described by the discrete probability distribution multiplied by the space volume. The expectation and variance of Poisson$(h_i(t))$ both equal to the rate of occurrence $h_i(t)$. Additionally, the molecules released by the local generator also follows the Fick's second law. Therefore, the number of the molecule released by the local generator, $N_b(t)$, also follows a Poisson distribution with rate of occurrence $h_l(t)$, that is

$$\frac{N_b(t)}{V_{space}} \sim \text{Poisson}\left(h_l(t)\right). \tag{40}$$

Since the number of molecules release by the transmitter is often huge, by the central limit theorem, the Poisson distribution can be approximated by a Gaussian distribution whose mean and variance equal to the rate of occurrence, i.e.,

$$\frac{N_a(t)}{V_{space}} \sim N\left(h_i(t), h_i(t)\right) \tag{41}$$

$$\frac{N_b(t)}{V_{space}} \sim N\left(h_l(t), h_l(t)\right), \tag{42}$$

where $N(\mu, \sigma^2)$ denotes a Gaussian distribution with mean μ and variance σ^2. From (2), MPD computes the difference between the two concentrations without considering the effect of counting noise. Under the assumption that counting noises for both signals are independent and Gaussian, we have

$$\frac{N_c(t)}{V_{space}} = \frac{N_a(t) - N_b(t)}{V_{space}} \sim N(h_i(t) - h_l(t), h_i(t) + h_l(t)), \tag{43}$$

where $N_c(t) \equiv N_a(t) - N_b(t)$.As the MPLL is locked, $h_i(t) - h_l(t)$ approaches to zero and (43) becomes

$$\frac{N_c(t)}{V_{space}} \sim N\left(0, h_i(t) + h_l(t)\right). \tag{44}$$

Figs. 11 and 12 demonstrate the numerical effects of counting noise with variance 1% for the S curve of the MPD and for the locally generated signal, respectively. As shown in Fig. 11, the ideal operation of the MPD is drawn as the linear red line, while the MPD operation with the effect of the molecule counting noise is represented as the blue curve. Due to the Gaussian-distributed counting noise in (43), the MPD operation deviates from the ideal case. Further, the slope of the linear range is slightly deeper than that of the ideal case at the cost of a shorter linear range. Thus, counting noise would significantly affect the

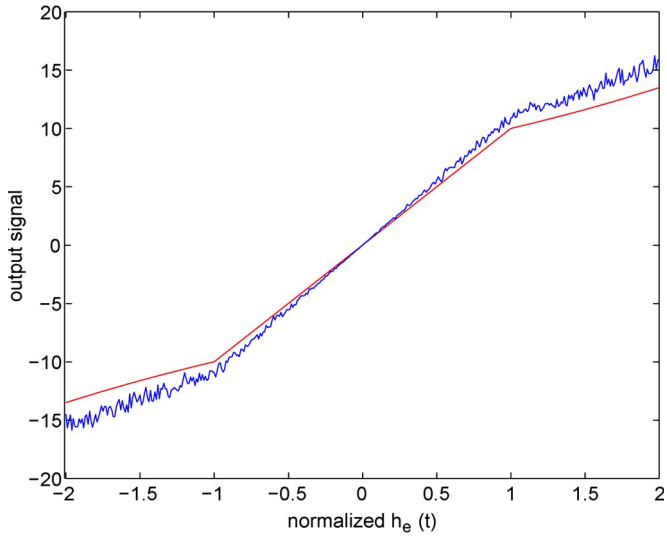

Fig. 11. S curve of phase detector, where the red line is the ideal operation of the phase detector and the blue line is with the molecule counting noise.

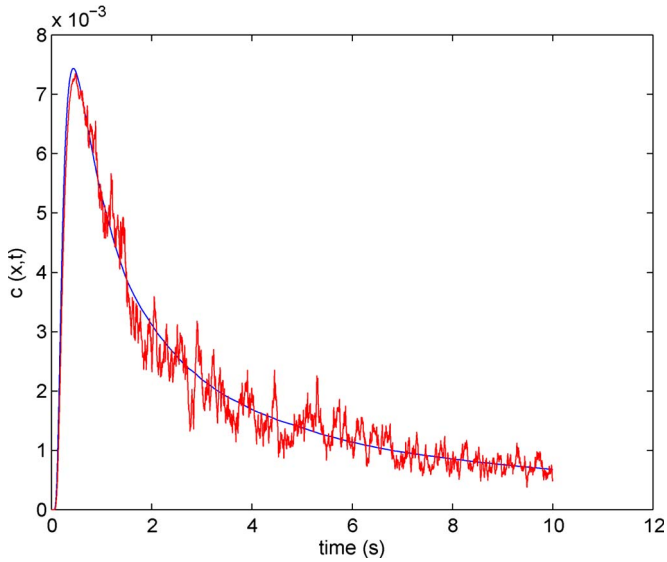

Fig. 12. Molecule counting noise, where the red line corresponds to locally generated signal h_l and the blue line is the input signal h_i.

behavior of the MPLL and deteriorates the operational range of the MPD. Fig. 12 shows the effect of counting noise to the locally generated signal. At the beginning, the loop is in-tracked fast. After both the locally generated signal (red curve) and the input signal (blue curve) reach their peaks, the variance of the error signal $h_i(x,t) - h_l(x,t)$ causes the locally generated signal deviate from the in-tracked condition. This deviation lasts until both the input and locally generated signal fade to small values, compared to their peak values. Subsequently, this locally generated signal would affect the output of the MPD, $h_e(x,t)$ and would drive the system out of stability.

Based on our analytical and numerical investigations, the notable behavior of MPLL can be summarized as follows:

- The compensation of the net charges among the heterogeneous reacting molecules in MPLL is analogous to the synchronization to align timing or phase among input and locally generated signals in a classic PLL.
- Since reacting molecules diffuse through fluid mediums and react slowly; thus, several issues (e.g., displacement (36) and counting error (43), which can be ignored in a classic PLL must be taken in to consideration in a MPLL.
- The diffusion coefficient is a critical issue affecting the MPLL behavior in acquisition time, S-curve, and fluctuation in error signals, as shown in Fig. 7,. This coefficient can be determined by the chemical reactants, the property of fluid medium, and the reacting environments.
- The acquisition is affected by the diffusion coefficient, loop gain, propagation delay jitter, displacement deviation, and molecule counting noises. Among these effects, displacement deviation and molecule counting noise have more significant impacts, as depicted in Figs. 9–12.
- The loop gain would affect the error signal, the MPLL's acquisition time, and the stable situation, but the effect is not monotonically increasing or decreasing. For the quality of error signal, as shown in Fig. 3, a larger loop gain is preferable. While for the acquisition time, a moderate loop gain, say 0 to 20 dB, would shorten the acquisition time; but as the loop gain grows above 20 dB, the acquisition time grows. These observations make loop gain a critical factor in designing a MPLL.
- The PLL may be out of lock if (i) large displacement deviation, say 100% of the transmit-receive distance, exists, and/or (ii) significant molecule counting noise appears at a moderate loop gain, say 10 dB, is utilized.
- If the implementation complexity is a concern, we shall investment more computing power on the adjustment of displacement and on the precision of molecule counting/measurement.

VI. Conclusion

A molecular PLL is proposed and analyzed for diffusion-based molecular communication systems and computing systems. The model is based on the Fick's second law for the diffusion process and the principles of a classic phase-locked loop. Each element of the MPLL is well specified and important characteristics, including steady-state error, loop gain, S-curve, and acquisition are rigorously analyzed. The stochastic behaviors like jitter performance, displacement issue, and the effect of molecule counting noise are examined in this research. Numerical results for the whole MPLL performance are given in both ideal and noisy cases. Finally, this pioneer investigation on MPLL enables a key component of molecular computing and communication. However, further discussions of the molecular PLL, like a three-dimensional diffusion process, higher-order loops, multiple input sources, and other propagation factors (more than radiation) in realistic experiments are still wanted toward realization of molecular communication systems.

Acknowledgment

The authors greatly appreciate constructive suggestions of anonymous reviewers and the third author thank Prof. Po-Lin Kuo's discussion to inspire his original design.

REFERENCES

[1] I. Yamashita, K. Iwahori, and S. Kumagai, "Ferritin in the field of nanodevices," *Biochimica et Biophys. Acta (BBA)-Gen. Subjects*, vol. 1800, no. 8, pp. 846–857, Aug. 2010.

[2] R. A. Freitas, *Nanomedicine, Volume I: Basic Capabilities*, T. Georgetown, Ed. Austin, TX, USA: Landes Biosci., 1999.

[3] I. F. Akyildiz, F. Brunetti, and C. Blazquez, "Nanonetworks: A new communication paradigm at molecular level," *Comput. Netw. (Elsevier) J.*, vol. 52, no. 12, pp. 2260–2279, Aug. 2008.

[4] M. Pierobon and I. F. Akyildiz, "A physical end-to-end model for molecular communication in nanonetworks," *IEEE J. Sel. Area Commun.*, vol. 28, no. 4, pp. 602–611, May 2010.

[5] P.-C. Yeh *et al.*, "A new frontier of wireless communication theory: Diffusion-based molecular communications," *IEEE Wireless Commun.*, vol. 19, no. 5, pp. 28–35, Oct. 2012.

[6] S. Hiyama *et al.*, "Molecular communication," in *Proc. NSTI Nanotechnol.*, Anaheim, CA, USA, 2005, pp. 391–394.

[7] V. Balzani, A. Credi, and M. Venturi, "Molecular devices and machines," *Nanotoday*, vol. 2, no. 2, pp. 18–25, Apr. 2007.

[8] A. Cavalcanti, "Assembly automation with evolutionary nanorobots and sensor-based control applied to nanomedicine," *IEEE Trans. Nanotechnol.*, vol. 2, no. 2, pp. 82–87, 2003.

[9] B. Atakan and O. B. Akan, "Body area nanonetworks with molecular communications in nanomedicine," *IEEE Commun. Mag.*, vol. 50, no. 1, pp. 28–34, Jan. 2012.

[10] T. Nakano, M. Moore, F. Wei, A. Vasilakos, and J. Shuai, "Molecular communication and networking: Opportunities and challenges," *IEEE Trans Nanobiosci.*, vol. 11, no. 2, pp. 135–148, Jun. 2012.

[11] M. J. Moore and T. Nakano, "Oscillation and synchronization of molecular machines by the diffusion of inhibitory molecules," *IEEE Trans. Nanotechnol.*, vol. 12, no. 4, pp. 601–608, Jul. 2013.

[12] C. M. Waters and B. L. Bassler, "Quorum sensing: Cell-to-cell communication in bacteria," *Annu. Rev. Cell Develop. Biol.*, vol. 21, pp. 319–346, Nov. 2005.

[13] M. Elowitz and S. Leibler, "A synthetic oscillatory network of transcriptional regulators," *Nature*, vol. 403, pp. 335–338, Jan. 2000.

[14] M. Heinemann and S. Panke, "Synthetic biology putting engineering into biology," *Bioinformatics*, vol. 22, no. 22, pp. 2790–2799, 2006.

[15] T. Bulter *et al.*, "Design of artificial cell-cell communications using gene and metabolic networks," *Proc. Nat. Acad. Sci.*, vol. 101, no. 8, pp. 2299–2304, Feb. 2004.

[16] A. Taylor, M. Tinsley, F. Wang, Z. Huang, and K. Showalter, "Dynamic quorum sensing and synchronization in large population of chemical oscillators," *Science*, vol. 323, pp. 614–617, 2009.

[17] T. Danino, O. Mondragon-Palomino, L. Tsimring, and J. Hasty, "A synthetic oscillatory network of transcriptional regulators," *Nature*, vol. 463, pp. 326–330, 2010.

[18] J. Goutsias and G. Jenkinson, "Markovian dynamics on complex reaction networks," *Phys. Rep.*, vol. 529, no. 2, pp. 199–264, Aug. 2013.

[19] A. J. Viterbi, *Principles of Coherent Communication*. New York, NY, USA: McGraw-Hill, 1966.

[20] K. V. Srinivas, R. S. Adve, and A. W. Eckford, "Molecular communication in fluid media: The additive inverse Gaussian noise channel," *IEEE Trans. Inf. Theory*, vol. 58, no. 7, pp. 4678–4692, Jul. 2012.

[21] M. Pierobon and I. F. Akyildiz, "Diffusion-based noise analysis for molecular communication in nanonetworks," *IEEE Trans. Signal Process.*, vol. 59, no. 6, pp. 2532–2547, Jun. 2011.

[22] M. Moore, T. Suda, and K. Oiwa, "Molecular communication: Modeling noise effects on information rate," *IEEE Trans Nanobiosci.*, vol. 8, no. 2, pp. 169–180, Jun. 2009.

[23] T. Nakano and L. Jian-Qin, "Design and analysis of molecular relay channels: An information theoretic approach," *IEEE Trans. Nanobiosci.*, vol. 9, no. 3, pp. 213–221, Sep. 2010.

[24] T. Nakano and M. Moore, "In-sequence molecule delivery over an aqueous medium," *Nano Commun. Netw.*, vol. 1, no. 3, pp. 181–188, Sep. 2010.

[25] B. Atakan and O. B. Akan, "On channel capacity and error compensation in molecular communication," *Trans. Comput. Syst. Biol.*, vol. 5410, pp. 59–80, Feb. 2008.

[26] B. Atakan and O. B. Akan, "Deterministic capacity of information flow in molecular nanonetworks," *Nano Commun. Netw.*, vol. 1, no. 1, pp. 31–42, Mar. 2010.

[27] B. Atakan, S. Galms, and O. B. Akan, "Nanoscale communication with molecular arrays in nanonetworks," *IEEE Trans. Nanobiosci.*, vol. 11, no. 2, pp. 149–160, Jun. 2012.

[28] T. Suda, M. Moore, T. Nakano, R. Egashira, and A. Enomoto, "Exploratory research on molecular communication between nanomachines," in *Proc. GECCO*, 2005, pp. 1–5.

[29] L.-S. Meng, P.-C. Yeh, K.-C. Chen, and I. F. Akyildiz, "A diffusion-based binary digital communication system," in *Proc. IEEE ICC*, Ottawa, Canada, 2012, pp. 4985–4989.

[30] E. L. Cussler, *Diffusion. Mass Transfer in Fluid Systems*, 2nd ed. Cambridge, U.K.: Cambridge Univ. Press, 1997.

[31] Y. Ali and L. Zhang, "Relativistic heat conduction," *Int. J. Heat Mass Transfer*, vol. 48, pp. 2397–2406, 2005.

[32] K.-C. Chen and L. D. Davisson, "Analysis of a new bit tracking loop-SCcl," *IEEE Trans. Commun.*, vol. 40, no. 1, pp. 199–209, 1992.

[33] P. Waage and C. Gulberg, "Studies concerning affinity," *J. Chem. Edu.*, vol. 63, no. 12, p. 1044, Dec. 1986.

[34] A. Kolmogorofl, I. Petrovsky, and N. Piscounofl, "A study of the diffusion equation with growth of the quantity of matter and its application to a biology problem," *Bull. Moscow Univ. Math. Ser. A*, vol. 1, no. 6, pp. 1–25, 1937.

[35] W. Ma and B. Fuchssteiner, "Explicit and exact solutions to a kolmogorov-petrovskii-piskunov equation," *Int. J. Non-Linear Mech.*, vol. 31, no. 3, pp. 329–338, 1996.

Chieh Lo received the B.S. degree in electrical engineering from the National Taiwan University, Taipei, Taiwan, in 2013. He is currently in a one-year mandatory military service in Taiwan. He will join Carnegie Mellon University, Pittsburg, PA, USA, in Fall 2014 working toward the Ph.D. degree. His research interests include molecular communications and mathematical modeling and analysis.

Yao-Jen Liang (M'11) received the B.S. degree in electronics engineering from National Chiao Tung University, Hsinchu, Taiwan, in 1994, and the M.S. degree in electrical engineering and the Ph.D. degree in communication engineering from National Taiwan University, Taipei, Taiwan, in 1996 and 2010, respectively.

He has more than six years experience in industry. From 2010 to 2011, he was a Postdoctoral Fellow at the Institute of Information Science, Academia Sinica, Taiwan. From February 2011 to February 2012, he was a Visiting Scholar at the School of Electrical and Computer Engineering, Georgia Institute of Technology. He is currently an Assistant Professor with the Department of Electrical Engineering, National Chiayi University. His current research interests include MIMO and OFDM systems, statistical signal processing, and molecular communications.

Kwang-Cheng Chen (M'89–SM'94–F'07) received the B.S. degree from the National Taiwan University, Taipei, Taiwan, in 1983, and the M.S. and Ph.D degrees from the University of Maryland, College Park, MD, USA, in 1987 and 1989, all in electrical engineering. From 1987 to 1998, he worked with SSE, COMSAT, IBM Thomas J. Watson Research Center, and National Tsing Hua University, in mobile communications and networks. Since 1998, he has been with National Taiwan University, Taipei, Taiwan, ROC, and is the Distinguished Professor and Associate Dean for academic affairs at the College of Electrical Engineering and Computer Science, National Taiwan University. During 2013–2014, he is also a SKKU Fellow Professor, Korea. His recent research interests include wireless communications, network science, and data analytics. He has been actively involved in the organization of various IEEE conferences as General/TPC chair/co-chair, and has served in editorships with a few IEEE journals. He also actively participates in and has contributed essential technology to various IEEE 802, Bluetooth, and 3GPP wireless standards. He has authored and co-authored over 200 IEEE papers and more than 20 granted US patents. He co-edited (with R. DeMarca) the book *Mobile WiMAX* (Wiley, 2008), and authored the book *Principles of Communications* (River, 2009) and co-authored (with R. Prasad) the book *Cognitive Radio Networks* (Wiley, 2009). He has received a number of awards including the 2011 IEEE COMSOC WTC Recognition Award. He has co-authored a few award-winning IEEE papers, including the 2014 IEEE Jack Neubauer Memorial Award.